

Capillary Flotation in a System of Two Immiscible Bose-Einstein Condensates

Victor P. Ruban*

*Landau Institute for Theoretical Physics RAS,
Chernogolovka, Moscow region, 142432 Russia*

(Dated: September 3, 2021)

A spatially inhomogeneous, trapped two-component Bose-Einstein condensate of cold atoms in the phase separation mode has been numerically simulated. It has been demonstrated for the first time that the surface tension between the components makes possible the existence of drops of a denser phase floating on the surface of a less dense phase. Depending on the harmonic trap anisotropy and other system parameters, a stable equilibrium of the drop is achieved either at the poles or at the equator. The drop flotation sometimes persists even in the presence of an attached quantized vortex.

I. INTRODUCTION

Multicomponent mixtures of ultracold Bose-Einstein condensed atomic gases have been studied for twenty-five years [1-5]. Such systems consist either of different chemical (alkaline) elements or of different isotopes of the same element, or of the same isotopes in two different internal (hyperfine) quantum states. Interactions between components lead to a variety of phenomena that are absent in simple Bose-Einstein condensates. In this case, it is essential that the parameters of nonlinear interactions between matter waves, proportional to the corresponding scattering lengths, in many cases can be changed over a wide range using Feshbach resonances [6-10]. In particular, a sufficiently strong cross-repulsion between the two types of atoms results in spatial separation of condensates [11, 12] and in the presence of an effective surface tension on the domain walls between the phases [4, 13]. This separation is responsible for many interesting configurations and phenomena such as a nontrivial geometry of the ground state of binary immiscible Bose-Einstein condensates in traps [14-16] (including optical lattices [17-19]), bubble dynamics [20], quantum analogs of classical hydrodynamic instabilities (Kelvin-Helmholtz [21, 22], Rayleigh-Taylor [23-25], Plateau-Rayleigh [26]), parametric instability of capillary waves at the interface [27, 28], complex textures in rotating binary condensates [29-31], core filled vortices [3, 32-37], three-dimensional topological structures [38-43], etc.

Large-scale dynamics of the interface in a separated binary condensate is very similar to the dynamics of bubbles and drops in the classical mechanics of immiscible ideal fluids [20, 23-25]. In the absence of quantized vortices, the flow is potential inside each of the components, and the entire vorticity of the velocity field is concentrated at the interface. In this sense, the bubble boundary is a vortex sheet similar to vortex sheets in $^3\text{He-A}$ in some cases [44]. Such structures also play an important role in turbulence (see [45-47] and references therein).

Note that the analogy with classical hydrodynamics

has not yet been exhausted. In particular, in the presence of a sufficiently strong surface tension, a moderate drop of a denser fluid can float on the surface of a less dense fluid. As far as I know, such capillary flotation in the case of binary condensates has not yet been investigated. The aim of this work is to numerically demonstrate the possibility of a heavy drop to float within the framework of the system of coupled Gross-Pitaevskii equations (1) and (2) describing a dilute Bose-Einstein condensate at zero temperature. Contrary to ordinary nearly incompressible fluids in a homogeneous gravitational field, we will consider Bose-Einstein condensates in a trap with a quadratic anisotropic potential, so that the equilibrium profile of a less dense fluid $\rho_{\text{eq}}(\mathbf{r})$ [see Eq.(6)] will be strongly inhomogeneous in space. In this case, the surface tension is proportional to $\rho_{\text{eq}}^{3/2}$ [13]; i.e., it is absent on the Thomas-Fermi surface and increases deeper into the condensate. Moreover, since the Thomas-Fermi surface has the form of an oblate or prolate ellipsoid of revolution, the effective potential energy of a drop depends not only on the locally vertical deviation of its center of mass but also on two local horizontal coordinates on the ellipsoid. As a result, the drop can oscillate along the “latitudinal” coordinate of the ellipsoid during its swimming. Depending on the system parameters, the horizontal potential energy minimum can be achieved either at the poles or at the equator of the ellipsoid.

II. MODEL AND NUMERICAL METHOD

The essence of the phenomenon can be demonstrated for the simplest case with equal masses of both types of atoms $m_1 = m_2 = m$, which approximately includes the case of a small difference in isotope masses, for example, ^{85}Rb and ^{87}Rb . Let an axisymmetric harmonic trap be characterized by a transverse frequency ω_{\perp} and anisotropy $\lambda = \omega_{\parallel}/\omega_{\perp}$. Choosing scales $\tau = 1/\omega_{\perp}$ for time, $l_{\text{tr}} = \sqrt{\hbar/\omega_{\perp}m}$ for length, and $\varepsilon = \hbar\omega_{\perp}$ for energy, dimensionless equations of motion for the complex wavefunctions $A(\mathbf{r}, t)$ and $B(\mathbf{r}, t)$ can be written in the

*Electronic address: ruban@itp.ac.ru

form

$$i\dot{A} = -\frac{1}{2}\nabla^2 A + [V(x, y, z) + g_{11}|A|^2 + g_{12}|B|^2] A, \quad (1)$$

$$i\dot{B} = -\frac{1}{2}\nabla^2 B + [V(x, y, z) + g_{21}|A|^2 + g_{22}|B|^2] B, \quad (2)$$

where $V = (x^2 + y^2 + \lambda^2 z^2)/2$ is the potential of the trap and $g_{\alpha\beta}$ is the symmetric matrix of nonlinear interactions (in our case, with positive elements). Physical interactions are determined by scattering lengths $a_{\alpha\beta}$ [2]:

$$g_{\alpha\beta}^{\text{phys}} = 2\pi\hbar^2 a_{\alpha\beta} (m_\alpha^{-1} + m_\beta^{-1}). \quad (3)$$

Without loss of generality, the first self-repulsion coefficient can be set to $g_{11} = 1$, since $g_{\alpha\beta}$ are considered to be fixed parameters (in each numerical experiment) in this work.

The conserved numbers of trapped atoms are given by the formulas

$$N_1 = \frac{l_{\text{tr}}}{4\pi a_{11}} \int |A|^2 d^3\mathbf{r} = (l_{\text{tr}}/a_{11})n_1, \quad (4)$$

$$N_2 = \frac{l_{\text{tr}}}{4\pi a_{11}} \int |B|^2 d^3\mathbf{r} = (l_{\text{tr}}/a_{11})n_2. \quad (5)$$

In real experiments, the ratio l_{tr}/a_{11} is in the range from several hundred to several thousand.

The simple model specified by Eqs. (1) and (2) is conservative. It is applicable only in the zero-temperature limit and cannot describe any finite-temperature effects (including dissipative effects). For comparison, the equations of motion for, e.g., ^3He [48] are more complex, and thermodynamics is of great importance.

The system of Eqs. (1) and (2) describes in essence a two-fluid ideal hydrodynamics (when both velocity fields are potential), with the difference that the total pressure of each component consists of the normal hydrodynamic pressure and the so-called quantum pressure. Quantum pressure only appears where the density changes drastically in space. In our case, this is a transition layer. The hydrodynamic pressures of both fluids are $g_{11}|A|^4/2$ and $g_{22}|B|^4/2$, so that, at equal pressures, the component with the lower self-repulsion coefficient is denser. For definiteness, it is assumed that $g_{22} < g_{11} = 1$; i.e., a relatively small drop of the denser second phase will float on the free surface of the first phase owing to the surface tension.

The background density profile of the first component is characterized by the chemical potential μ . For $\mu \gg 1$, in the Thomas-Fermi approximation, one obtains

$$|A_0|^2 \approx [\mu - V(x, y, z)] \equiv \mu\rho_{\text{eq}}(\mathbf{r}). \quad (6)$$

Thus, the effective transverse radius of the condensate is $R = \sqrt{2\mu}$, and the longitudinal half-size is $Z = \lambda R$.

The phase separation condition has the form $g = (g_{12}^2 - g_{11}g_{22}) > 0$ [11, 12]. There is a narrow transition layer between separated condensates, where the densities of both phases decrease to almost zero in one or the

other direction. In this case, the corresponding excess of energy (surface tension coefficient) is determined by a formula $\sigma = F(g_{22}/g_{11}, g_{12}/g_{11})|A_0|^3$ [11, 13]. In contrast to ordinary incompressible fluids, the dependence of the surface tension on the background density is very significant here.

The numerical modeling carried out in this work was focused on experimentally implemented mixtures ^{85}Rb - ^{87}Rb [8], where $a_{12}/a_{22} \approx 2$, while a_{11} can be changed over a wide range using the Feshbach resonance. Therefore, in all our numerical experiments, $g_{12} = 2g_{22}$. There were different values for g_{22} , including $g_{22} = 0.6, 0.7, 0.8$.

The used numerical method was quite standard and included two procedures. The first procedure is the preparation of the initial state by applying (to an arbitrary “input” state) gradient descent, which in this case is equivalent to imaginary time propagation on a finite interval of an auxiliary quasi-time variable. This dissipative procedure filtered out fast excitations and left only the soft modes that did not reach their minimum energy. A quasi-equilibrium transition layer was also formed between the phases. The second procedure is the actual modeling of the system of Eqs. (1) and (2) using the second-order split-step Fourier method with periodic boundary conditions in spatial coordinates. In general, the numerical method is similar to that used in [49].

III. RESULTS

A natural tendency toward an increase in the maximum possible mass of a floating drop with a decrease in the relative difference between g_{11} and g_{22} was observed.

Some of the numerical results are demonstrated in Figs.1-3. For clarity, in the first and second examples, the configurations are chosen symmetric with respect to the $y = 0$ plane. The total density profiles in this plane indicate the presence of a relatively denser drop near the surface as well as a transition layer between the components.

Fig.1 illustrates the case where the poles are stable positions of the drop on the ellipsoid. It oscillates slowly around its high point (see video [50]). It should be mentioned that a drop with a greater mass ($n_2 = 45$) is no longer able to adhere to the surface and instead undergoes complex motions inside the ellipsoid, sometimes remaining near the surface for a short time (see video [51]).

Fig.2 corresponds to a smaller relative difference in the densities of the two phases compared to the first example. In this case, the effective potential energy of a floating drop reaches a local minimum at the equator (see video [52]). In this example, the drop is sufficiently large and is deformed noticeably during its motion. Note that, in the case of a prolate ellipsoid with anisotropy $\lambda = 0.7$, the poles are stable positions of such a drop (not presented here). Apparently, the difference in behavior is due to different natures of the dependences of curvature of the Thomas-Fermi surface and the local “gravity” on

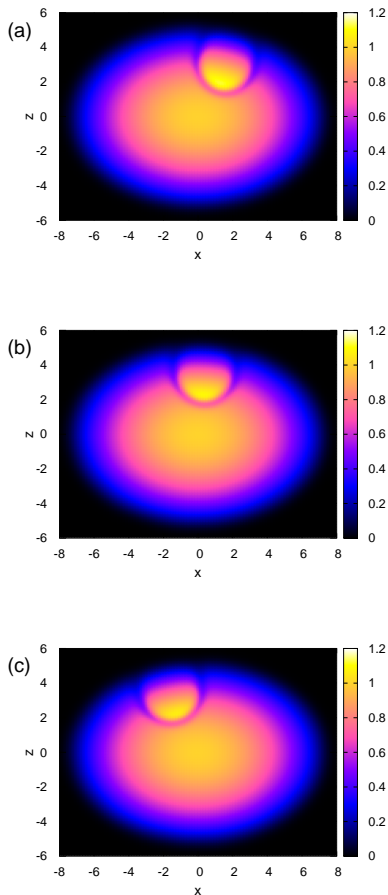


Figure 1: Total density map of two condensates normalized to μ in the $y = 0$ plane for a floating heavy drop obtained numerically with the parameters $\lambda = 1.4$, $g_{11} = 1.0$, $g_{22} = 0.7$, $g_{12} = 1.4$, $n_1 = 1282.4$, $n_2 = 37.1$, and $\mu = 30$ for the times $t =$ (a) 500, (b) 600, and (c) 700. The drop undergoes slow oscillations near the pole, and panels (a) and (c) correspond approximately to its extreme positions.

the polar angle. This is however a problematic question, since for, e.g., $g_{22} = 0.7$ (the same as in Fig.1) the prolate ellipsoid still attracts the drop to the pole (not shown). More research is required here.

It is interesting that a drop can also remain floating when a quantized vortex passing through the first component is attached to it (compare with [43], where a large dense drop is located in the center of the system and stabilizes several attached vortex filaments by its mass). In the example shown in Fig.3, the drop does not sink, although the vortex creates an additional force pulling it down (see video [53]). A more massive drop with $n_2 = 49.0$ under similar conditions moves up and down repeatedly along the vortex from pole to pole through the entire condensate (see video [54]).

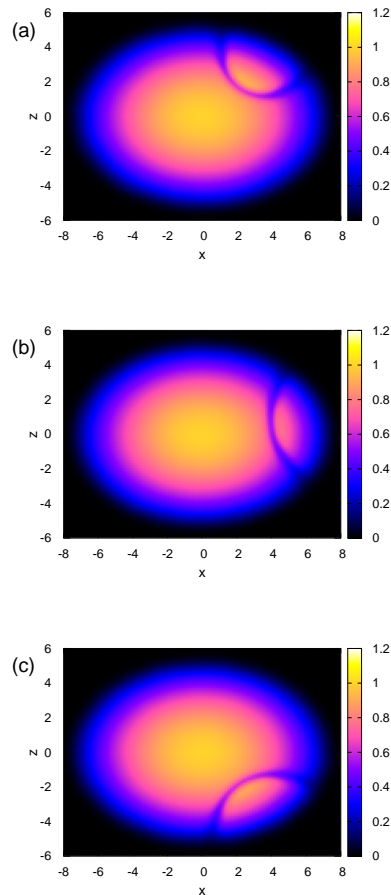


Figure 2: Total density map of two condensates normalized to μ in the $y = 0$ plane for a floating drop oscillating near the equator. The drop is less dense, larger, and more mobile than that in Fig.1. It is obtained numerically with the parameters $\lambda = 1.4$, $g_{11} = 1.0$, $g_{22} = 0.8$, $g_{12} = 1.6$, $n_1 = 1270.8$, $n_2 = 50.2$, and $\mu = 30$ for the times $t =$ (a) 680, (b) 700, and (c) 720. Panels (a) and (c) correspond approximately to the extreme positions of the drop.

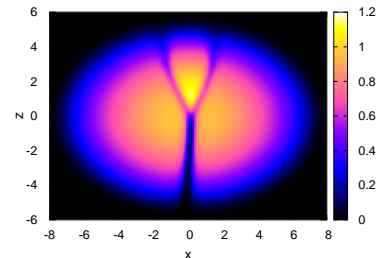


Figure 3: Total density map of a floating drop with an attached quantized vortex in the $y = 0$ plane obtained numerically with the parameters $\lambda = 1.4$, $g_{11} = 1.0$, $g_{22} = 0.8$, $g_{12} = 1.6$, $n_1 = 1275.5$, $n_2 = 28.9$, and $\mu = 30$ for the time $t = 300$.

IV. CONCLUSIONS

To summarize, analogous to ordinary drops floating on the surface of a less dense fluid in a gravity field owing to the surface tension, floating quantum drops in a system of two immiscible trapped Bose-Einstein condensates have been numerically detected. An essential difference is the

absence of a neutral equilibrium of a quantum drop in coordinates along the Thomas-Fermi surface. This effect is obviously due to the finiteness of the drop size compared to the size of the main phase. An approximate analytical calculation of the corresponding dependence of the drop potential energy and its equilibrium geometric shape remains an interesting problem for further investigation.

-
- [1] Tin-Lun Ho and V. B. Shenoy, Phys. Rev. Lett. **77**, 3276 (1996).
- [2] H. Pu and N. P. Bigelow, Phys. Rev. Lett. **80**, 1130 (1998).
- [3] B. P. Anderson, P. C. Haljan, C. E. Wieman, and E. A. Cornell, Phys. Rev. Lett. **85**, 2857 (2000).
- [4] S. Coen and M. Haelterman, Phys. Rev. Lett. **87**, 140401 (2001).
- [5] G. Modugno, M. Modugno, F. Riboli, G. Roati, and M. Inguscio, Phys. Rev. Lett. **89**, 190404 (2002).
- [6] J. P. Burke, Jr., J. L. Bohn, B. D. Esry, and C. H. Greene, Phys. Rev. Lett. **80**, 2097 (1998).
- [7] G. Thalhammer, G. Barontini, L. De Sarlo, J. Catani, F. Minardi, and M. Inguscio, Phys. Rev. Lett. **100**, 210402 (2008).
- [8] S. B. Papp, J. M. Pino, and C. E. Wieman, Phys. Rev. Lett. **101**, 040402 (2008).
- [9] S. Tojo, Y. Taguchi, Y. Masuyama, T. Hayashi, H. Saito, and T. Hirano, Phys. Rev. A **82**, 033609 (2010).
- [10] C. Chin, R. Grimm, P. Julienne, and E. Tiesinga, Rev. Mod. Phys. **82**, 1225 (2010).
- [11] E. Timmermans, Phys. Rev. Lett. **81**, 5718 (1998).
- [12] P. Ao and S. T. Chui, Phys. Rev. A **58**, 4836 (1998).
- [13] B. Van Schaeybroeck, Phys. Rev. A **78**, 023624 (2008).
- [14] A. A. Svidzinsky and S. T. Chui, Phys. Rev. A **68**, (2003).
- [15] S. Gautam and D. Angom, J. Phys. B: At. Mol. Opt. Phys. **43**, 095302 (2010).
- [16] R. W. Pattinson, T. P. Billam, S. A. Gardiner, D. J. McCarron, H. W. Cho, S. L. Cornish, N. G. Parker, and N. P. Proukakis, Phys. Rev. A **87**, 013625 (2013).
- [17] K. Suthar, Arko Roy, and D. Angom, Phys. Rev. A **91**, 043615 (2015).
- [18] K. Suthar and D. Angom, Phys. Rev. A **93**, 063608 (2016).
- [19] K. Suthar and D. Angom, Phys. Rev. A **95**, 043602 (2017).
- [20] K. Sasaki, N. Suzuki, and H. Saito, Phys. Rev. A **83**, 033602 (2011).
- [21] H. Takeuchi, N. Suzuki, K. Kasamatsu, H. Saito, and M. Tsubota, Phys. Rev. B **81**, 094517 (2010).
- [22] N. Suzuki, H. Takeuchi, K. Kasamatsu, M. Tsubota, and H. Saito, Phys. Rev. A **82**, 063604 (2010).
- [23] K. Sasaki, N. Suzuki, D. Akamatsu, and H. Saito, Phys. Rev. A **80**, 063611 (2009).
- [24] S. Gautam and D. Angom, Phys. Rev. A **81**, 053616 (2010).
- [25] T. Kadokura, T. Aioi, K. Sasaki, T. Kishimoto, and H. Saito, Phys. Rev. A **85**, 013602 (2012).
- [26] K. Sasaki, N. Suzuki, and H. Saito, Phys. Rev. A **83**, 053606 (2011).
- [27] D. Kobyakov, V. Bychkov, E. Lundh, A. Bezett, and M. Marklund, Phys. Rev. A **86**, 023614 (2012).
- [28] D. K. Maity, K. Mukherjee, S. I. Mistakidis, S. Das, P. G. Kevrekidis, S. Majumder, and P. Schmelcher, Phys. Rev. A **102**, 033320, (2020).
- [29] K. Kasamatsu, M. Tsubota, and M. Ueda, Phys. Rev. Lett. **91**, 150406 (2003).
- [30] K. Kasamatsu and M. Tsubota, Phys. Rev. A **79**, 023606 (2009).
- [31] P. Mason and A. Aftalion, Phys. Rev. A **84**, 033611 (2011).
- [32] K. J. H. Law, P. G. Kevrekidis, and L. S. Tuckerman, Phys. Rev. Lett. **105**, 160405 (2010); *Erratum*, Phys. Rev. Lett. **106**, 199903 (2011).
- [33] M. Pola, J. Stockhofe, P. Schmelcher, and P. G. Kevrekidis, Phys. Rev. A **86**, 053601 (2012).
- [34] S. Hayashi, M. Tsubota, and H. Takeuchi, Phys. Rev. A **87**, 063628 (2013).
- [35] A. Richaud, V. Penna, R. Mayol, and M. Guilleumas, Phys. Rev. A **101**, 013630 (2020).
- [36] A. Richaud, V. Penna, and A. L. Fetter, Phys. Rev. A **103**, 023311 (2021).
- [37] V. P. Ruban, JETP Lett. **113**, 532 (2021).
- [38] K. Kasamatsu, M. Tsubota, and M. Ueda, Phys. Rev. Lett. **93**, 250406 (2004).
- [39] H. Takeuchi, K. Kasamatsu, M. Tsubota, and M. Nitta, Phys. Rev. Lett. **109**, 245301 (2012).
- [40] M. Nitta, K. Kasamatsu, M. Tsubota, and H. Takeuchi, Phys. Rev. A **85**, 053639 (2012).
- [41] K. Kasamatsu, H. Takeuchi, M. Tsubota, and M. Nitta, Phys. Rev. A **88**, 013620 (2013).
- [42] S. B. Gudnason and M. Nitta, Phys. Rev. D **98**, 125002 (2018).
- [43] V. P. Ruban, arXiv:2104.05296.
- [44] G. E. Volovik, Phys. Usp. **58**, 897 (2015).
- [45] D. S. Agafontsev, E. A. Kuznetsov, and A. A. Mailybaev, Phys. Fluids **30**, 095104 (2018).
- [46] E. A. Kuznetov and E. V. Sereshchenko, JETP Lett. **109**, 239 (2019).
- [47] A. Migdal, Intl. J. Modern Phys. A **36**, 2150062 (2021).
- [48] M. M. Salomaa and G. E. Volovik, Rev. Mod. Phys. **59**, 533 (1987).
- [49] V. P. Ruban, JETP Lett. **108**, 605 (2018).
- [50] <http://home.itp.ac.ru/~ruban/20MAY2021/V1Y.avi>
- [51] <http://home.itp.ac.ru/~ruban/20MAY2021/V1N.avi>
- [52] <http://home.itp.ac.ru/~ruban/20MAY2021/V2Y.avi>
- [53] <http://home.itp.ac.ru/~ruban/20MAY2021/V3Y.avi>
- [54] <http://home.itp.ac.ru/~ruban/20MAY2021/V3N.avi>